SLOPE SCALE ESTIMATES OF CRACK PROPAGATION SPEEDS FROM AVALANCHE VIDEOS

Ron Simenhois[1*], Karl W. Birkeland[2, 3], Johan Gaume[4, 5], Alec van Herwijnen[4], Bastian Bergfeld[4], Bertil Trottet[6], Ethan Greene[1]

[1]*Colorado Avalanche Information Center, Boulder, CO, USA*
[2]*Friends of the Colorado Avalanche Information Center*
[3]*Birkeland Snow and Avalanche Scientific, Bozeman, MT, USA*
[4]*WSL Institute for Snow and Avalanche Research SLF, Davos, Switzerland*
[5]*Alpine Mass Movements, ETH Zürich*
[6]*École Polytechnique Fédérale de Lausanne, Lausanne, Switzerland*

ABSTRACT: Dry-snow slab avalanches release due to crack propagation in a weak snow layer under a cohesive snow slab. Crack propagation speeds along the weak layer provide insights into the potential size of avalanches, information on the fracture regime, and affirm avalanche release models. Despite their importance, slope-scale crack speed measurements from real avalanches are limited. Further, most existing slope-scale measurements rely on the appearance of slab fractures on the snow surface, which occur following weak layer fracture. Here, we present a novel method to estimate crack propagation speed from snow surface movements in avalanche videos. Our technique uses changes in pixel intensity, allowing us to detect the location of the crack in the weak layer well before slab fractures appear on the snow surface. We used field experiments and numerical simulations to validate our method before applying it to videos of real avalanches. Our results show that cracks propagate faster up and down the slope than in the cross-slope direction, suggesting that different regimes govern crack growth depending on propagation direction.

KEYWORDS: Avalanche, slab, weak layer, crack, speed, video

1. INTRODUCTION

Dry-snow slab avalanches result from a sequence of fracture processes. First, weak layer failure initiates under a cohesive slab, resulting in a localized crack. Second, once that crack expands to a critical size, crack propagation begins. Third, the crack extends across the slope, a process called dynamic crack propagation. Finally, avalanche release occurs if the tangential component of the gravitational load due to the slab overcomes frictional resistance to sliding. Eventually, cracks initiate at the avalanche's crown, flanks, and stauchwall (Schweizer et al., 2003; Schweizer et al., 2016).

Spatial variations in slab and weak layer properties play a crucial role in determining the behavior of cracks during the dynamic crack propagation phase. Specifically, these variations can lead to fracture arrest in certain localized areas with stronger weak layers. This occurs when the energy required to extend the crack surpasses the energy released during crack extension (Jamieson and Johnston, 1992; Gaume et al., 2015). However, if these local variations are not significant enough, the kinetic energy of the propagating crack can overcome the energy deficit, enabling continued crack propagation (Broberg, 1996). Consequently, the crack propagation speed becomes a critical factor influencing the crack propagation distance.

Observations from video analyses of Propagation Saw Tests (PSTs) (Gauthier and Jamieson, 2006) indicate that faster propagating cracks tend to travel longer distances (van Herwijnen et al., 2016). Nevertheless, the underlying reason for the correlation between crack speed and propagation distance remains incompletely understood.

* *Corresponding author address:*
Ron Simenhois, Colorado Avalanche Information Center;
tel: +1 303-818-4876
email: ron.simenhois@state.co.us

Despite the significance of crack speed (Gross and Seelig, 2017), relatively few direct measurements exist over distances exceeding a few meters or in actual avalanche start zones. Johnson and others (2004) made one of the first direct measurements of crack speed, using geophones in flat terrain to measure a crack speed of 20 +/-2 m/s over 8 meters. van Herwijnen and Jamieson (2005) reported similar speeds on isolated beams, with values ranging between 17 and 26 m/s. Crack propagation speed measurements made with high-speed videos of PSTs combined with particle tracking velocimetry (PTV) range from 10 to 50 m/s (van Herwijnen and Birkeland, 2014; van Herwijnen and Jamieson, 2005; van Herwijnen et al., 2016; Bair et al., 2014.). van Herwijnen and Schweizer (2011) used a seismic sensor array to estimate a crack speed of 42 +/- 4 m/s for an avalanche that was 60 meters wide in Switzerland, and van Herwijnen (2005) analyzed 11 avalanche videos to calculate speeds ranging from 15 to 32 m/s. Similar speed values were also reported based on numerical simulations of the PST (Gaume et al., 2015). More recently, Bergfeld et al. (2022) used synchronized accelerometers to measure a crack propagation speed of 49 +/-5 m/s over 25 meters of flat terrain. Bergfeld et al. (2021) and Bergfeld et al. (2018) used Digital Image Correlation (DIC) to measure crack speeds between 20 and 30 m/s and between 37 and 45 m/s, respectively, in 3.3 m PSTs. Bergfeld et al. (2023) used DIC again to measure crack propagation speeds on long PST experiments (up to 9 m long) over the entire life cycle of a weak layer. They measured speeds as fast as 55 +/-8 m/s. Hamre et al. (2014) analyzed videos of avalanches to estimate crack speeds that were much faster. Some of their crack speeds approached 200 m/s, with an average speed of 80 m/s for 27 videos.

Crack speed estimates from PSTs, collapsing weak layers on flat terrain, and cross-slope propagation in avalanches and numerical models are limited by the flexural wave speed of the slab (Bergfeld et al., 2021) and align with theoretical predictions of incipient shear cracks of 29–41 m/s (McClung, 2005) and asymptotic flexural speeds of 21 - 26 m/s (Heierli et al., 2008). However, the much higher speeds in some avalanches estimated by Hamre et al. (2014) contradict those theoretical predictions. Recent modeling by Gaume et al. (2018; 2019), Trottet et al. (2022), and Bobillier et al. (2022) suggested that the processes governing crack propagation vary between flat terrain and in different directions on slopes. Their speed estimates on low-angle terrain align with those from theoretical models and experimental measurements. However, on slopes steeper than the snow friction angle, they report a transition from relatively slower anticrack propagation to much faster supershear crack propagation with supersonic speed regarding the slab's Rayleigh wave speed but subsonic regarding the slab's p-wave speeds. Thus far, few crack speed measurements on real slope-scale avalanches exist to verify these model predictions. There have been many weak layer crack speed measurements, but most are on low-angle terrain or at scales smaller than a typical avalanche starting zone (<5 m).

Except for the avalanche measured by van Herwijnen and Schweizer (2011), all experimental crack speeds measured at a larger scale on steep slopes are indirect crack speed measurements relying on video frame measurements of visible surface cracks (van Herwijnen and Jamieson, 2005; Hamre et al., 2014; Bergfeld et al., 2021). Bergfeld et al. (2021) suggest the error associated with this method becomes negligible for large avalanches (≤5% crack propagation speed for crack propagation over 200 m). However, this technique is limited because videos of such large crack propagations are rare and are typically in the cross-slope direction.

Recently, Simenhois and others (2023) presented the Elurian Video Detection (EVD) - a new method that allows tracking snow surface movements resulting from weak layer crack propagation before visible cracks appear on the snow surface (Figure 1). Here, we summarize their results with an additional estimate of an explosive-triggered avalanche from Southeast Alaska and the theoretical implications as well as practical developments for avalanche risk management.

2. METHODS

2.1 Video processing

Our method follows those used by Simenhois et al. (2023). In short, we assume that the most significant changes in pixel intensity within the start zone and between the time of initiation to just before the appearance of cracks on the snow surface are due to snow surface

movement associated with weak layer fracture. We then follow a four-step process where, in the first step, we stabilize the video to where each point (x, y) in the video sequence points to the same location in the slope. In the second step,

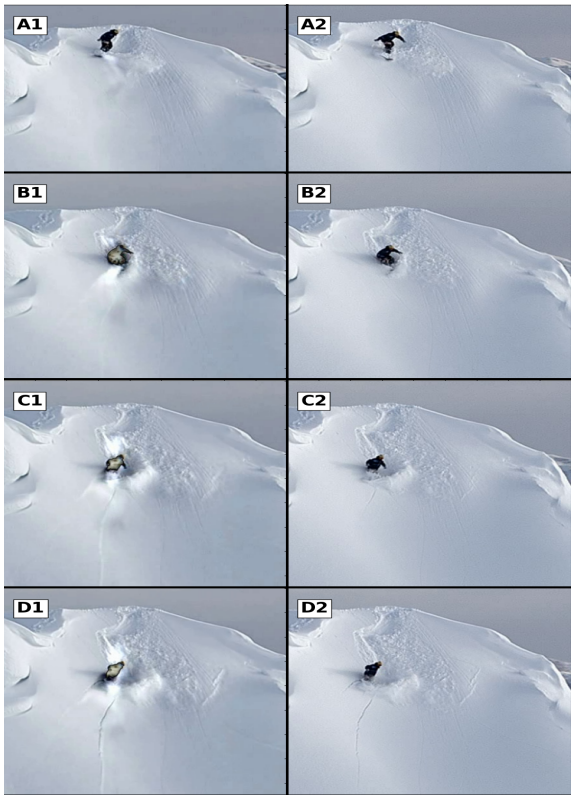

Figure 1: Comparison of enhanced (left) and original (right) frames extracted from a video of an avalanche from Alaska. We estimate that the crack in the weak layer was initiated at frame number 38. At frame number 37 (row A, 0.04 s. before crack initiation), snow surface movement from the snowboarder pushing the snow surface is visible up to 1.5 m downslope from the snowboarder. Frame number 47 (row B, 0.18 s. after crack initiation), snow surface movement is visible downslope from the snowboarder in the enhanced images (B1). Cracks on the snow surface below the snowboarder appear on frame 52 (C2, 0.28 s. after crack initiation), and snow surface movement becomes visible where the crown wall eventually develops to the left of the snowboarder (C1). In frame 56 (row D, 0.36 s. after crack initiation), the crown wall starts to appear on the snow surface in the original video (D2) (Figure from Simenhois et al., 2023).

we use principles of the Eulerian Video Magnification (Wu et al., 2012), where we first applied a spatial decomposition Gaussian pyramid (Burt and Adelson, 1983) to each video frame. Second, we use a temporal filter for the frame sequence. Third, we apply the reversed spatial decomposition of step one, and finally, we detect spatial and temporal changes in intensity for each pixel in the up-sampled frame sequence (Figure 2).

2.2 Crack speed estimates and analysis

We had the exact location of the avalanche for two of our avalanche videos. We geo-located the avalanche slope to derive the distances from the crack initiation to the detected locations of slab motion. We estimated the skier/snowboarder height for the other four videos to be 1.75 m. We calculated the distances between different locations on the slope by comparing these distances in pixels to the size of the snowboarder in pixel units. We estimated our distance measurement error to be +/ – 10 pixels and our time error to be +/- two video frames. In addition, we assumed that the crack tips travel away from the initiation point; thus, we omitted the detected location that appeared in the same direction as the initiation point after another detected location further away.

To differentiate between slope and cross-slope direction crack propagation, we use the direction of the avalanche flow in the starting zone as the downslope direction. We considered propagation in direction to detected points within 45° of the slope direction (up or down) as slope direction and the rest as cross-slope direction.

In our analysis, we also differentiated between hard and soft slab avalanches. As a rough measure, we considered an avalanche a hard slab when avalanche debris blocks remained larger than a third of a person while traveling through the avalanche starting zone. We classified the rest of the avalanches as soft slabs.

2.2 Method verification

We verified the accuracy of our method by comparing speed estimates to measurements

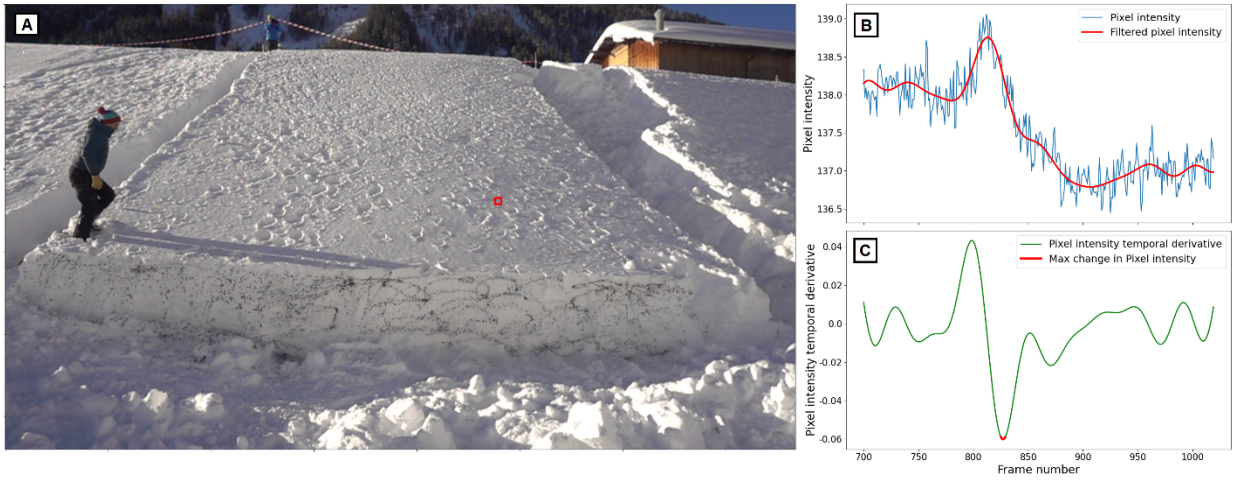

Figure 2: A) A video frame of a 10 m by 10 m avalanche release. B) The pixel intensity (in blue) and the filtered signal (in red) of the pixels in the red rectangle. C) The first temporal derivative of the filtered pixel intensity signal. The derivative minima (red dot) at frame 828 represented when the weak layer's crack passed below the area marked with the red rectangle. Both (B) and (C) share the same x-axis. (Figure from Simenhois et al., 2023).

from Particle Tracking Velocimetry (PTV) (Crocker and Grier, 1996;, van Herwijnen et al., 2016), Digital Image Correlation (DIC), and Material Point Method (MPM) simulation of physically-based render (PBR) with Houdini software (See Simenhois et al., 2023 for more verification methods and results). In addition, we compare time and space detection of snow surface movements between the snow surface and weak layer fracture on an exposed wall in a small avalanche experiment.

3. RESULTS

3.1 Method verification

Our detection of snow surface movement and the crack tip in the small avalanche experiment shows that both detected snow surface movements and crack tip are tracking closely in time and space (Figure 3).

3.2 Slope-scale crack speed estimates

We analyzed five skier or snowboarder-triggered avalanches and one explosive-triggered avalanche. We classified four of the avalanches as hard slab avalanches and two as soft slab avalanches. In these videos, the slab hardness and the direction of crack propagation with respect to the slope affected weak layer crack speeds. We observed snow surface movement rapidly advancing in the up- and down-slope directions (Figure 4) with slower snow surface movement in the cross-slope direction. Crack speeds in the slope direction averaged 138 m/s, while cross-slope crack speeds were considerably lower, averaging 34 m/s. Thus, slope-direction crack speeds averaged nearly four times faster than cross-slope crack speeds (Figure 5). Mean estimated crack speeds in hard slab avalanches were 1.6 and 1.7 times faster than soft slab avalanches in cross-slope and slope directions, respectively (Figure 5). We did have two notable outliers in our down-slope crack speeds, with estimates of 26 and 29 m/sec. However, these estimates were less than 15 m from the crack initiation point. Our measurements suggest that down-slope crack speeds close to the initiation point (within about 15 m) and cross-slope crack speeds align reasonably well with previous speed estimates measured for PSTs and whumpfs (van Herwijnen and Birkeland, 2014; van Herwijnen, 2005; Bair et al., 2014; Bergfeld et al., 2021; Bergfeld et al., 2023), and cross-slope speeds estimated for larger avalanches (Bergfeld et al., 2022). Please see Simenhois et al. (2023) for more comprehensive results.

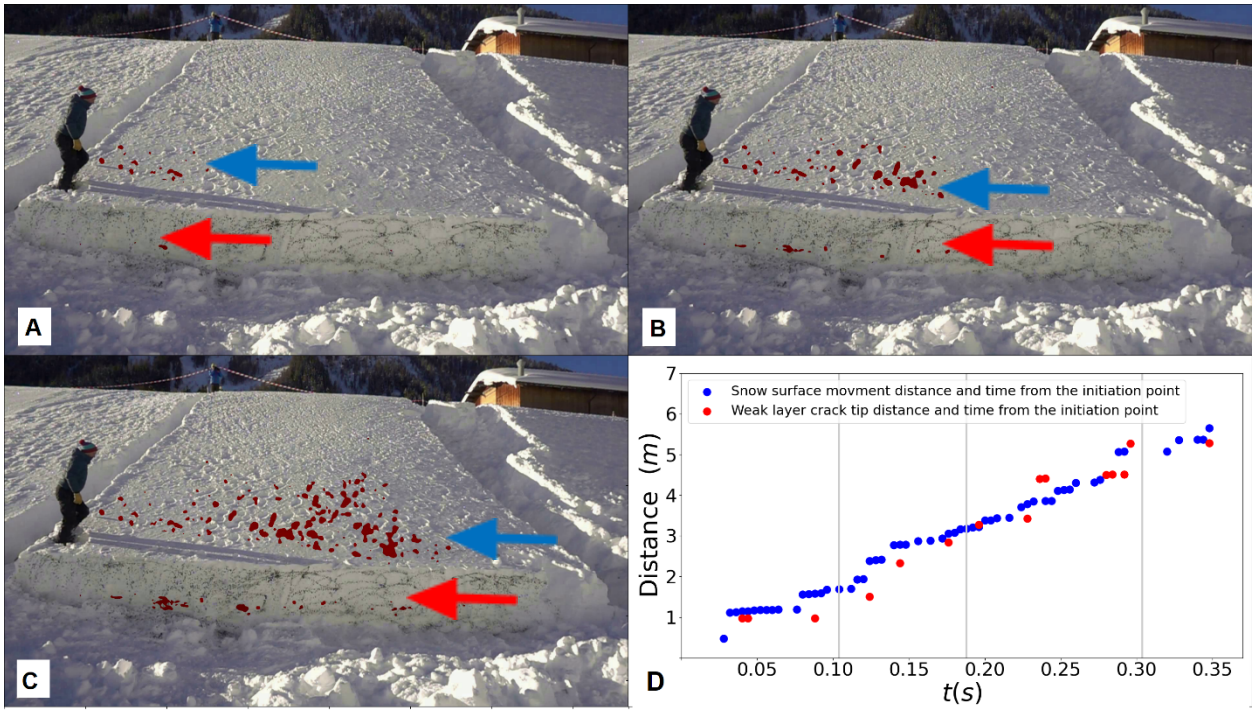

Figure 3: A sequence of video frames where both snow surface movements (marked in blue arrow) and weak layer cracks have been detected (marked in red arrow) after 0.1 seconds (A), 0.18 seconds (B), and 0.3 seconds (C). D: Distance and time from the initiation point and time for both detected snow surface motion (blue) and detected weak layer crack tip (red). The gray vertical lines in D show the time of frames A, B, and C (Figure from Simenhois et al., 2023).

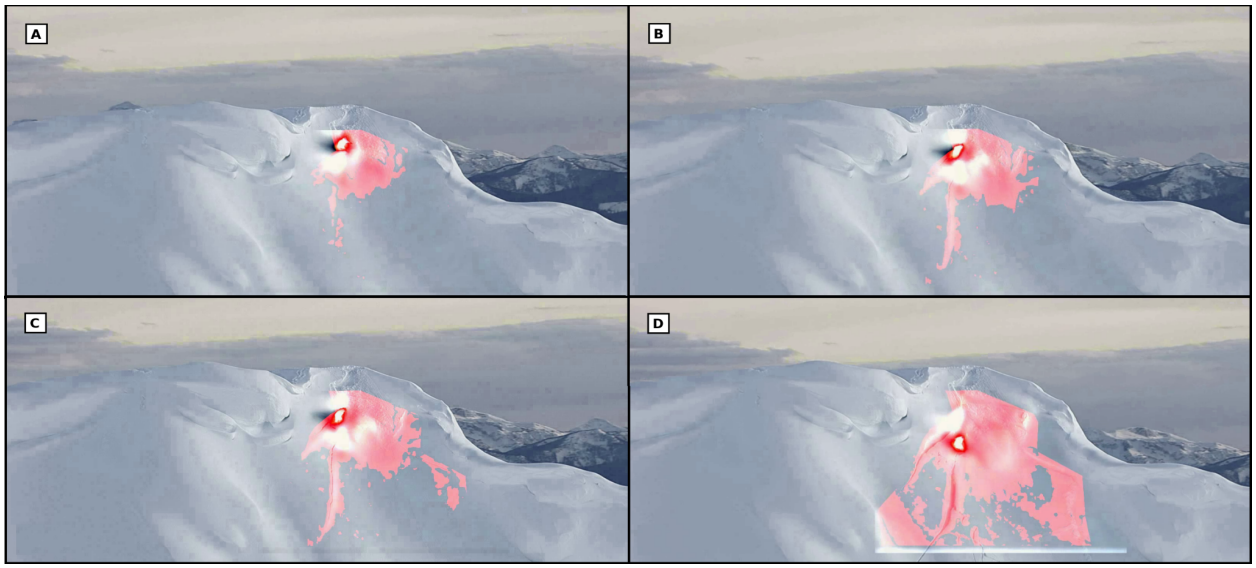

Figure 4: A sequence of video frames of avalanche release. In red are the locations where we detected snow surface movement up to the time of the frame. Initially (A and B), weak layer crack propagation can only be detected advancing downslope from the snowboarder. As larger areas of the weak layer fractured downslope from the snowboarder, crack propagation advances in the cross-slope direction. (Figure from Simenhois et al., 2023)

Table 1: Mean speed estimates from the six videos (from Simehois et al., 2023).

Location	*Slab Hardness*	*Trigger*	*Direction*	*Mean Speed (m/s)*
Alaska1	Soft Slab	Snowboarding	Downslope	56
			Cross slope	17
Alaska2	Soft Slab	Snowboarding	Downslope	138
			Cross slope	29
Alaska3	Hard Slab	Explosive	Downslope	163
			Cross slope	38
France	Hard Slab	Skiing	Downslope	141
			Cross slope	37
Switzerland1	Hard Slab	Landing	Downslope	194
			Cross slope	52
Switzerland2	Hard Slab	Landing	Upslope	132
			Cross slope	29

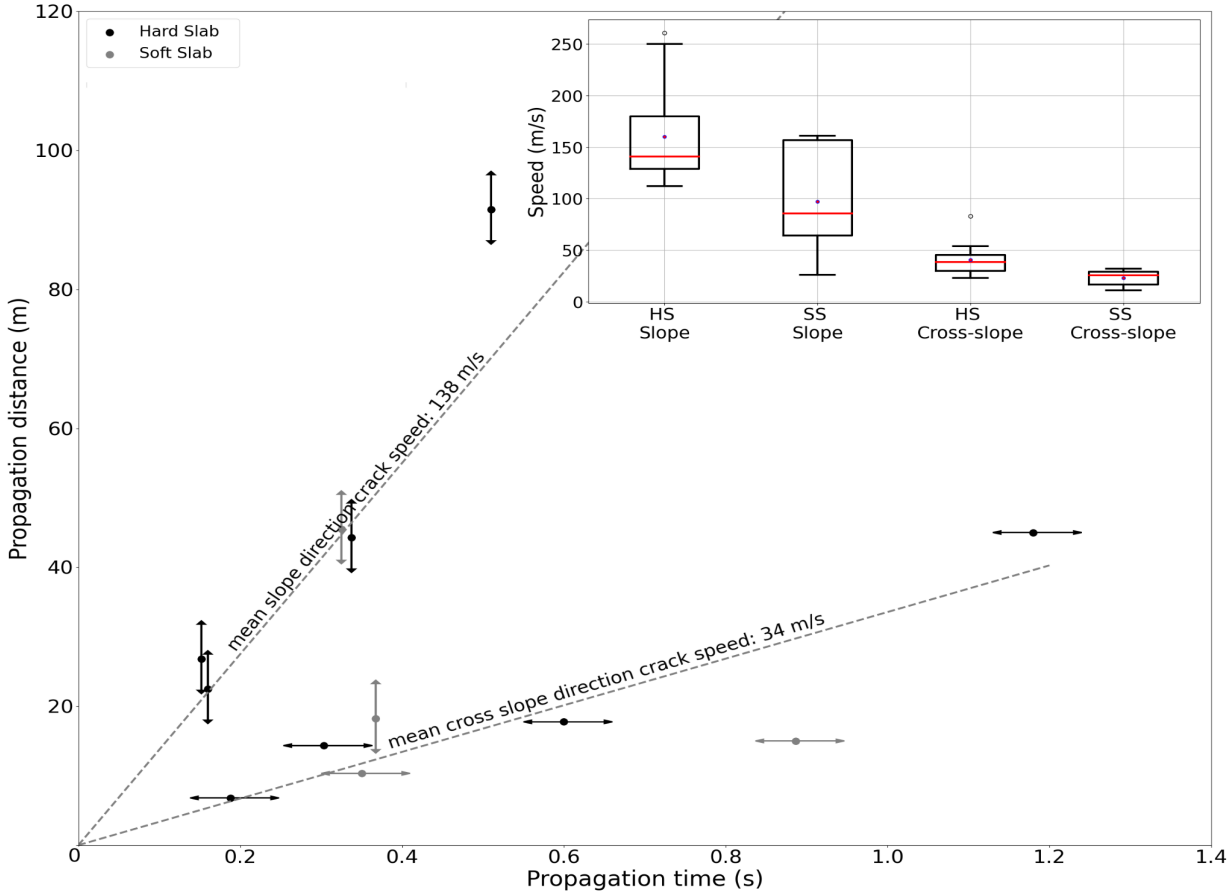

Figure 5. Representation of the mean values for each avalanche. The arrows represent the direction of propagation (slope and cross slope), and the colors represent slab hardness (hard slab in black, and soft slab in gray). The dashed lines' steepness represents the mean speed for the direction of propagation. The box plot in the upper right side shows the crack speeds by propagation direction and slab hardness. We see faster propagating cracks in the slope direction compared to the cross-slope direction and faster-propagating cracks under harder slabs. (Figure modified from Simenhois et al., 2023)

4. DISCUSSION

Our results comparing up- and down-slope crack speed estimates to cross-slope estimates support the idea that different crack propagation regimes drive propagation on flat, up- and down-slope, and cross-slope directions. Further evidence is provided by comparing up- and down-slope crack speeds close to the initiation point to crack speeds farther from the initiation point. Our crack speed estimates within about 15 m of the initiation point – regardless of slope orientation – are about 27 +/- 2 m/s, aligning closely with previous crack speed estimates of PSTs and whumps, which range from 17 to 42 m/s (Jamieson and Johnston, 1992; van Herwijnen and Birkeland, 2014; van Herwijnen and Jamieson, 2005; van Herwijnen et al., 2016; Bair et al., 2014; Bergfeld et al., 2022, 2023). At distances farther than 15 m from the initiation point, speeds up- and down-slope greatly exceed cross-slope speeds. Here, our up- and down-slope crack speeds averaged 150 +/- 11 m/s, nearly four times faster than the mean cross-slope speeds. These higher estimates are consistent with the upper end of previous slope scale estimates by Hamre et al. (2014), which were based on surface cracks and could, therefore, only assess speeds well away from trigger points. Our results thus support the recent work by Trottet et al. (2022) and Bobillier et al. (2023), who proposed that cracks propagate as sub-Rayleigh anticracks close to initiation points before transitioning to a much faster supershear mode in the up- and down-slope directions. Cross-slope cracks are mode III fractures, which, in theory, have their speeds limited by the slab's flexural wave speed (Burridge, 1973; Bergfeld et al., 2022).

Our results also suggest faster slope-scale crack speeds with harder – and presumably denser – slabs (Figure 5; Table 1). This finding is consistent with previous field measurements with PSTs (van Herwijnen and Birkeland, 2014; van Herwijnen et al., 2016; Birkeland et al., 2019), and it also provides field verification for numerical simulations of Trottet et al. (2022) and Bobillier et al. (2023).

Since we estimated crack speeds from videos, our methods have limitations. First, our speeds are not direct estimates. Rather, we use snow surface movement as a proxy for crack tip location. Second, crack distances for four of our six avalanche videos are estimated from the snowboarder/skier's height and not from direct measurements. Third, our method does not always detect the crack tip location; as a result, most of our estimates are bulk estimates and not point estimates. Fourth, we estimated speed from only six avalanches; though, we did ensure an even contribution of all the avalanches when comparing crack speed trends between hard and soft slabs and between slope-parallel and cross-slope directions. Finally, we found that our method did not work on videos taken on cloudy days, so we could not adequately analyze videos taken in cloudy conditions.

Apart from the limitations already highlighted, further research is necessary to gain a more comprehensive understanding of the lighting prerequisites of our method.

Despite the limitations, our technique aligned well with previous techniques for measuring crack speeds. This gives us confidence that our methods will enable researchers to better investigate and understand weak layer crack propagation under actual slope-scale avalanches. Combining our novel video analysis technique with additional field measurements of snowpack properties may help us predict slope-scale crack speeds. That information might allow us to better predict propagation distance and the size of expected avalanches. In addition, a better understanding of avalanche release and crack speeds can help us develop new approaches for designing cost-effective avalanche mitigation and avalanche defense systems.

5. CONCLUSIONS

We present a novel method for tracking snow surface movement in the early stages of dry slab avalanche release. Unlike previous video analyses of slope scale crack propagation, our method tracks snow surface movement over time and space *before* surface cracks are visible. It relies on the change in frame pixel intensity to infer the position of the crack tip in the weak layer. The method has been validated based on field experiments and numerical simulations. Our measurements show that crack speeds vary with the direction of propagation with respect to the slope and slab hardness. Our work is an important step towards a better understanding of fracture processes involved in

dry-snow slab avalanche release at the slope scale.

ACKNOWLEDGMENTS

We want to thank Melin Walet for her help with the DIC analysis of the small avalanche experiment and Spencer Logan and Kelsy Been for their insightful comments on this article.
Parts of this article and the figures were reproduced from Simenhois et al., 2023:
Simenhois, R., Birkeland, K., Gaume, J., van Herwijnen, A., Bergfeld, B., Trottet, B., & Greene, E. (2023). Using video detection of snow surface movements to estimate weak layer crack propagation speeds. *Annals of Glaciology,* 1-11. doi:10.1017/aog.2023.36

CODE SHARING

Our code is open-source code. It is available at https://github.com/ronimos/Crack-Speed-Videos

REFERENCES

Bair, E.H., R. Simenhois, A. van Herwijnen, and K.W. Birkeland. (2014). The influence of edge effects on crack propagation in snow stability tests. The Cryosphere 8 (4): 1407–1418.

Bergfeld, B., A. van Herwijnen, J. Dual. and J. Schweizer. (2018). Dynamic crack propagation in weak snowpack layers: insights from high-resolution, high-speed photography. Proceedings of the International Snow Science Workshop, Innsbruck, Austria, 2018.

Bergfeld, B., A. van Herwijnen, G. Bobillier, E. Larose, L. Moreau, B. Trottet, J. Gaume, J. Cathomen, J. Dual, and J. Schweizer. (2022). Crack propagation speeds in weak snowpack layers. Journal ofGlaciology 68 (269): 557–570.

Bergfeld, B,, A. van Herwijnen, G. Bobillier, P. L Rosendahl, P. Weißgraeber, V. Adam, J. Dual, and J. Schweizer. (2023). Temporal evolution of crack propagation characteristics in a weak snowpack layer: conditions of crack arrest and sustained propagation. Natural Hazards and Earth System Sciences, 23, 293–315, https://doi.org/10.5194/nhess-23-293-2023, 2023.

Bergfeld, B., A. van Herwijnen, B. Reuter, G. Bobillier, J. Dual, and J. Schweizer. (2021). Dynamic crack propagation in weak snowpack layers: insights from high-resolution, high-speed photography. The Cryosphere 15 (7): 3539–3553.

Broberg, KB. 1996. How fast can a crack go? Materials Science 32 (1): 80–86.

Boyat, A. K., & Joshi, B. K. (2015). A Review Paper: Noise Models in Digital Image Processing. ArXiv. /abs/1505.034

Burridge, R. Admissible speeds for plane-strain self-similar shear cracks with friction but lacking cohesion. Geophys. J. Int. **35**, 439–455 (1973).

Burt, P., and E. Adelson (1983), The Laplacian pyramid as a compact image code, IEEE Transactions on Communications, 31(4), 532-540, doi: 10.1109/TCOM.1983.1095851.

Cooley, J. W., & Tukey, J. W. (1965). An algorithm for the machine calculation of complex Fourier series. Mathematics of computation, 19(90), 297-301.

Crocker, J. C, and D. G Grier. (1996). Methods of digital video microscopy for colloidal studies. Journal of colloid and interface science 179 (1): 298–310.

Gaume, J., T Gast, J Teran, A. van Herwijnen, and C Jiang. (2018). Dynamic anticrack propagation in snow. Nature communications 9 (1): 1–10.

Gaume, J., A. van Herwijnen, G. Chambon, K. W Birkeland, and J. Schweizer. (2015). Modeling of crack propagation in weak snowpack layers using the discrete element method. The Cryosphere 9 (5): 1915–1932.

Gaume, J., A. van Herwijnen, T. Gast, J. Teran, and C. Jiang. (2019). Investigating the release and flow of snow avalanches at the slope-scale using a unified model based on the material point method. Cold Regions Science and Technology 168:102847.

Gauthier, D., & Jamieson, B. (2006). Towards a field test for fracture propagation propensity in weak snowpack layers. Journal of Glaciology, 52(176), 164-168.

Gregoire, B., Bastian, B., Johan, G., & Jürg, S. (2022). Numerical and experimental investigation of crack propagation regimes in large-scale snow fracture experiments. Technical report. Copernicus Meetings.

Bobillier, G., B. Bergfeld, J. Dual, J. Gaume, A. van Herwijnen, and J. Schweizer. "Numerical investigation of crack propagation regimes in snow fracture experiments." Granul. Matter, in review (2023).

Gross, D., & Seelig, T. (2017). Fracture mechanics: with an introduction to micromechanics. Springer.

Hamre., D., R. Simenhois, and K. Birkeland. (2014). Fracture speeds of triggered avalanches. In Proceedings ISSW, 174–178.

Heierli, J, P Gumbsch, and M. Zaiser. (2008). Anticrack nucleation as triggering mechanism for snow slab avalanches. Science 321 (5886): 240–243.

Heierli, J. (2005). Solitary fracture waves in metastable snow stratifications. Journal of Geophysical Research: Earth Surface 110 (F2).

Jamieson, JB, and CD Johnston. (1992). Snowpack characteristics associated with avalanche accidents. Canadian Geotechnical Journal 29 (5): 862–866.

Johnson, B Crane, J Bruce Jamieson, and Robert R Stewart. (2004). Seismic measurement of fracture speed in a weak snowpack layer. Cold Regions Science and Technology 40 (1-2): 41–45.

Lucas, Bruce D, T. Kanade, et al. (1981). An iterative image registration technique with an application to stereo vision. Vol. 81. Vancouver.

McClung, DM. (2005). Approximate estimates of fracture speeds for dry slab avalanches. Geophysical Research Letters 32 (8).

Romberg, J. K., Choi, H., & Baraniuk, R. G. (1999, October). Bayesian wavelet-domain image modeling using hidden Markov trees. In Proceedings 1999 International Conference on Image Processing (Cat. 99CH36348) (Vol. 1, pp. 158-162). IEEE.

Schweizer, J., J B. Jamieson, and M. Schneebeli. (2003). Snow avalanche formation. Reviews of Geophysics 41 (4).

Schweizer, J., B. Reuter, A. van Herwijnen, B. Richter, and J. Gaume. (2016). Temporal evolution of crack propagation propensity in snow in relation to slab and weak layer properties. The Cryosphere 10 (6): 2637–2653.

Shi, J., & Tomasi, C. (1994). Good features to track. (1994). Proceedings of IEEE Conference on Computer Vision and Pattern Recognition, 593-600.

Simenhois, R., Birkeland, K., Gaume, J., van Herwijnen, A., Bergfeld, B., Trottet, B., & Greene, E. (2023). Using video detection of snow surface movements to estimate weak layer crack propagation speeds. Annals of Glaciology, 1-11. doi:10.1017/aog.2023.36.

Swamy, S., & Kulkarni, P. K. (2020). A basic overview on image denoising techniques. Int. Res. J. Eng. Technol., 7(5), 850-857.

Trottet, B., Simenhois, R., Bobillier, G. et al. Transition from sub-Rayleigh anticrack to supershear crack propagation in snow avalanches. Nat. Phys. **18**, 1094–1098 (2022). https://doi.org/10.1038/s41567-022-01662-4

van Herwijnen, A, and KW Birkeland. (2014). Measurements of snow slab displacement in extended column tests and comparison with propagation saw tests. Cold regions science and technology 97:97–103.

van Herwijnen, A, and B Jamieson. (2005). High-speed photography of fractures in weak snowpack layers. Cold Regions Science and Technology 43 (1-2): 71–82.

van Herwijnen, A., and J. Schweizer. (2011). Seismic sensor array for monitoring an avalanche start zone: design, deployment and preliminary results. Journal of Glaciology 57 (202): 267–276.

van Herwijnen, A. F. (2005). Fractures in weak snowpack layers in relation to slab avalanche release. University of Calgary, Calgary, AB. doi:10.11575/PRISM/15350

van Herwijnen A, Bair EH, Birkeland KW, Reuter B, Simenhois R, Jamieson B, and Jürg Schweizer. (2016). Measuring the mechanical properties of snow relevant for dry-snow slab avalanche release using particle tracking velocimetry. In Proceedings ISSW, 397–404.

Wu, H. Y., Rubinstein, M., Shih, E., Guttag, J., Durand, F., & Freeman, W. (2012). Eulerian video magnification for revealing subtle changes in the world. ACM transactions on graphics (TOG), 31(4), 1-8.